ADAPTIVE INTELLIGENT MPPT CONTROLLER COMPARISON OF PHOTOVOLTAIC SYSTEM UNDER DIFFERENT WEATHER CONDITIONS of GHARDAIA SITE (SOUTH OF ALGERIA)

L. ZAGHBA [a,b], N. TERKI[b] , A.BORNI[a] , A.BOUCHAKOUR[a], BENBITOUR NÉE KHENNANE MESSAOUDA[a].

[a] Unité de Recherche Appliquée en Energies Renouvelables, URAER, Centre de Développement des Energies Renouvelables, CDER, 47133, Ghardaïa, Algeria

[1] layachi40@yahoo.fr

[b] Electrical Engineering Department, University of Biskra, Algeria

[2] t_nadjiba@yahoo.fr

Abstract*— this paper presents modeling and simulation of the photovoltaic system under MATLAB/Simulink. Firstly we started with the estimation of solar radiation using the model of Liu & Jordan, and then from hourly meteorological parameters of two data (sunlight and ambient temperature), we estimated the maximum hourly power produced by PV generator and buck-boost output converter using adaptive artificial intelligence techniques (fuzzy and Neuro-fuzzy MPPT controller) in the region of Ghardaia (South of Algeria). This approach is used to study the influence of rapidly changing irradiance level concerning performance of photovoltaic systems. From the simulation results, the Neuro-fuzzy MPPT controller approach can deliver more power and provides a response time response from the tracking system from the point of maximum power and pics lower than the fuzzy logic control.*

Keywords Ghardaia site; Neuro-fuzzy MPPT controller;MATLAB/Simulink; photovoltaic system.

I. INTRODUCTION

A significant number MPPT control technique have been developed since the 70s, starting with simple techniques like MPPT controllers based the state feedback control of the voltage and current [1], the controllers using more efficient algorithms for calculate the MPPT for GPV ,among the most technical: Perturb and Observe (P&O) and incremental inductance MPPT Algorithm . In recent years, more robust and intelligent control techniques were associated with MPPT control such as Fuzzy logic and Neuro - Fuzzy in order to increase the efficiency of solar panels. In this perspective, we present the different parts of a PV system, fuzzy MPPT control will be studied and compared to an MPPT control using Neuro- Fuzzy controller.

TABLE I *: Geographical coordinates*

Latitude	**32° 38'00'' N**
Longitude	**03°81'00''W**
Altitude	**450 m**

The site is located in Ghardaia about 600 km south of Algiers. Having the following coordinates, Latitude: 32°36' N, Longitude: 3°81' E and elevation of 450 m above sea level, this area is classified as an arid region. Based upon meteorological data the solar resources and temperatures are as follows: rate of sunny days varies between 77% and 80 % per year. The average daylight hours are approximately 5 hours in winter and up to 10 hours over the remaining seasons. The daily average irradiation on a horizontal surface varies between 6 kW/m2 per day and 7 kW/m2 /day [1][2][3][4].

1. Global irradiation on inclined estimated by Liu & Jordan model

A. Direct solar radiation

The direct solar radiation estimated on inclined surface without being diffused by the atmosphere is given by:

$$S_i = S_{oh} R_b \quad (1)$$

Where, S_{oh} and R_b are respectively the direct solar radiation measured on horizontal surface and the tilt factor [2]:

$$S_{oh} = A\sin(h)\exp\left(\frac{-1}{C\sin(h+2)}\right) \quad (2)$$

$$R_b = \frac{\cos(\emptyset - i)\cos(\delta)\cos(\omega) + \sin(\emptyset - i)\sin(\delta)}{\cos(\emptyset)\cos(\delta)\cos(\omega) + \sin(\emptyset)\sin(\delta)} \quad (3)$$

δ : Declination angle, *h*: height of the sun, ϕ: latitude, ω:hour angle and i: tilted angle.
With:

$$\delta = 23.45 \sin[\frac{360}{365}(\mathrm{N} + 284)] \quad (4)$$

$$\sin(h) = \cos(\delta)\cos(\emptyset)\cos(\omega) + \sin(\emptyset)\sin(\delta) \quad (5)$$

$$\omega = 15(12 - TSV) \quad (6)$$

B. Diffuse solar radiation

The equation of diffuse solar radiation given by Liu &Jordan model which takes into account the isotropic part of sky is**:**

$$D_i = D_{oh}(\frac{1+cos(i)}{2}) \quad (7)$$

Where, D__ is the diffuse solar radiation measured on horizontal plane.

$$D_{oh} = B(\sin(h)^{0.4} \quad (8)$$

A, B and C are constants which reflect the nature of the sky.

C. Reflected solar radiation

For an inclined plane, the reflected radiation can be expressed by:

$$D_{re} = \rho.(S_{oh} + D_{oh}).(\frac{1-\cos(i)}{2}) \quad (9)$$

ρ: Albedo.

The reflected solar component in a horizontal plane is zero.

D. Global solar radiation

The total solar radiation measured or estimated on a inclined plan is given by:

$$G = S_i + D_i + D_{re} \quad (10)$$

2. Mathematical Model of PV cell

L'équation caractérisant la courbe de variation courant-tension I-V est donnée par [4-5]:

$$I = I_{ph} - I_s\left(exp^{\frac{V+IR_S}{V_t n}} - 1\right) - \frac{V+IR_S}{R_{sh}} \quad (11)$$

I_{ph} : courant de photo-génération ;
I_s : courant de saturation de la diode 1.
n: le facteur de qualité de la diode 1.
R_S = la résistance série.
R_{sh} = la résistance shunt.
Le courant photonique est lié à la température, l'éclairement et au courant photonique mesuré aux conditions de référence [6]:

$$I_{ph} = \frac{G}{G_{ref}}\left(I_{ph\,ref} - \mu_{cc}(T_c - T_{c\,ref})\right) \quad (12)$$

$I_{ph\,ref}$: Le courant photonique sous condition de référence.
μ_{cc} : Coefficient de sensibilité de l'intensité à la température.
$T_c, T_{c\,ref}$: Les températures de la cellule réelle et à la condition de référence.

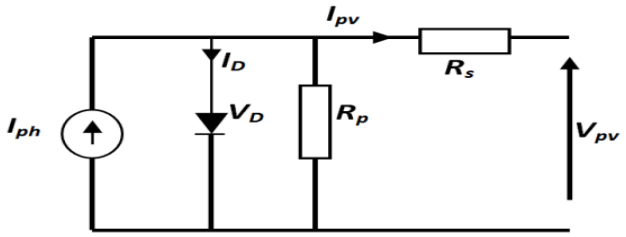

Fig.1 Typical circuit of PV solar cell.

3. Model of boost DC-DC converter

The schematic diagram of DC-DC boost converter connected to photovoltaic generator to a resistive load is shown in Fig.5 [1, 3, and 22]:

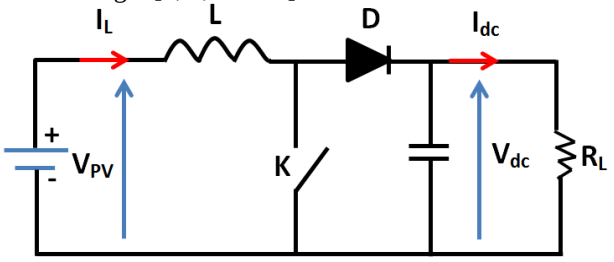

Fig.2 DC-DC Boost converter

The state-space averaged model of the boost converter can be written as:

$$\begin{bmatrix}\dot{\mathrm{I}}_{\mathrm{L}} \\ \dot{\mathrm{V}}_{\mathrm{dc}}\end{bmatrix} = \begin{bmatrix}0 & -\frac{1}{L}(1-u) \\ \frac{1}{C}(1-u) & -\frac{1}{C.R_L}\end{bmatrix}\begin{bmatrix}I_L \\ V_{dc}\end{bmatrix} + \begin{bmatrix}\frac{1}{L} \\ 0\end{bmatrix}V_{pv} \quad (13)$$

Where u is the duty cycle, V_{pv} is the input voltage to the boost converter, I_L is the inductor current, C is the capacitance, R_L is the load resistance and V_{dc} is the DC link output
The equation (13) can be written as:

$$\begin{cases}\dot{x}_1 = -\frac{1-u}{L}x_2 + \frac{1}{L}u \\ \dot{x}_2 = \frac{1-u}{C}x_1 + \frac{1}{RC}x_2\end{cases} \quad (14)$$

Where: $x = [I_L, V_c]$; $u: V_e$

4. Fuzzy logic MPPT controller

The FLC have the advantage to be robust and relatively simple to design as it does not require the knowledge of the exact model [9].
The proposed FLC, shown in Figure 3, has two inputs and one output which are the error e(k) and change of error de(k) at sampled times k [17][19].

$$e(k) = \frac{P_{pv}(k)-P_{pv}(k-1)}{V_{pv}(k)-V_{pv}(k-1)} \quad (15)$$

$$de(k) = e(k) - e(k-1) \quad (16)$$

Where: $P_{pv}(k)$ and $V_{pv}(k)$ are respectively the instantaneous output powers and output voltage of the photovoltaic generator.
The input e(k) shows if the load operation point at the instant k is located on the left or on the right of the maximum power point on the PV characteristic, while the input dE(k) expresses the moving direction of this point.
The fuzzy inference is carried out by using Madani's method, (Table II), and the defuzzification uses the center of gravity to compute the output of this FLC which is the duty cycle:

$$D = \frac{\sum_{j=1}^{n} u\,(D_j) D_j}{\sum_{j=1}^{n} u\,(D_j)} \quad (17)$$

The control rules are indicated in Table II with e and dE as Inputs and D as the output.

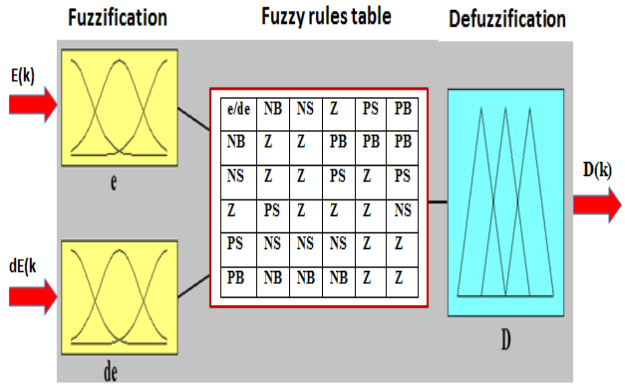

Fig.3 Structure of fuzzy controller

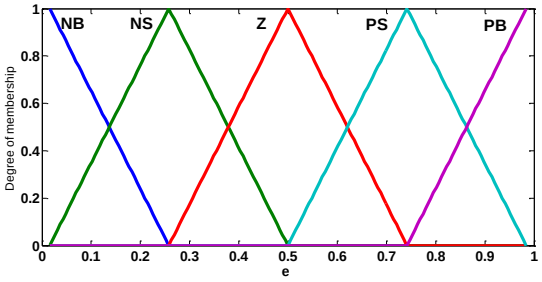

Fig.4. Membership function for error (e)

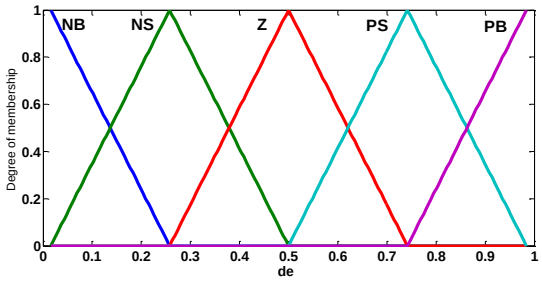

Fig.5. Membership function for change in error (de)

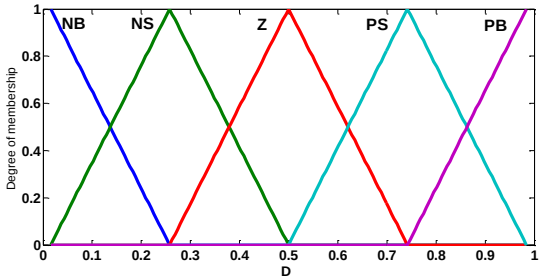

Fig.6. membership functions of output D (Duty cycler)

Table II *Fuzzy control rules*

e/de	NB	NS	Z	PS	PB
NB	Z	Z	PB	PB	PB
NS	Z	Z	PS	Z	PS
Z	PS	Z	Z	Z	NS
PS	NS	NS	NS	Z	Z
PB	NB	NB	NB	Z	Z

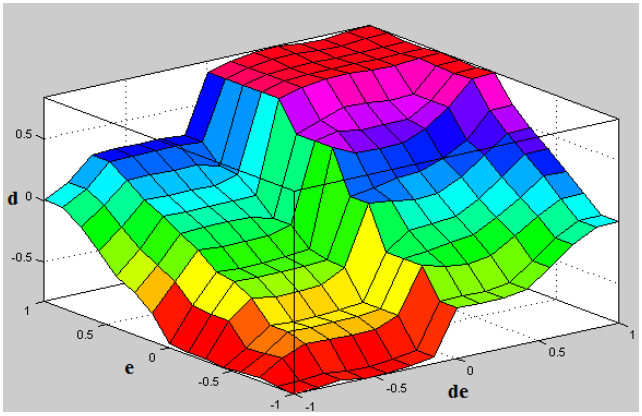

Fig.7 presentation of 3D (error e, error variation de and duty cycler d)

5. ANFIS MPPT controller

The adaptive network-based fuzzy inference systems (ANFIS) is used to solve problems related to parameter identification. This parameter identification is done through a hybrid learning rule combining the back-propagation gradient descent and a least-squares method. ANFIS is a hybridization strategy between two techniques:

neural networks, and fuzzy logic to develop a control system to tracking the maximum power point in order to extract the maximum power [18][20]. Figure 8 a shows the block diagram of a photovoltaic system with a MPPT control based neuro-fuzzy networks.

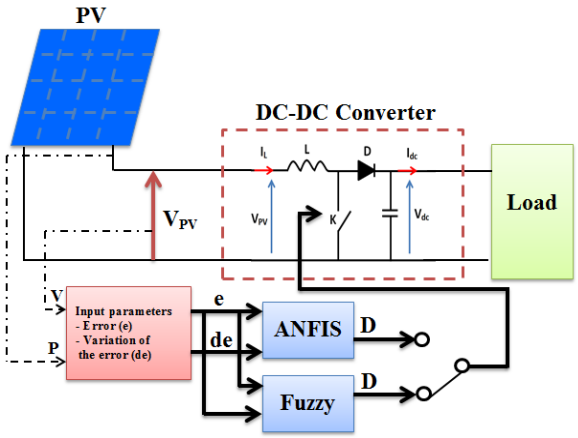

Fig. 8. Block diagram of PV Module with Fuzzy and ANFIS MPPT Controller

6. A. Description and structure of the proposed MPPT neuro-fuzzy controller

The neuro-fuzzy controller developed in this section has two input variables error (e) and the variation of the error (de) and a single output control (D). The two input variables produce the control action (D) to be applied to the DC-DC buck boost converter, in order to adjust the duty cycler ratio to ensure the adaptation of the power supplied by the GPV. ANFIS implements a Takagi - Sugeno type FIS and have an architecture composed of five layers as shown in Figure 9.

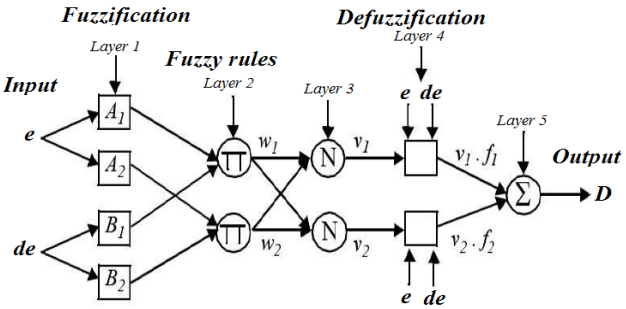

Fig.9 Architecture of the proposed ANFIS model.

A. Layer 1: consists of adaptive nodes that generate membership grades of linguistic labels based upon premise signals, using any appropriate parameterized membership function such as the generalized bell function.

$$O_i^1 = \mu_{Ai}(x) = \exp\left[\left(\frac{x-c_i}{a_i}\right)^2\right]^{bi} \qquad (18)$$

Where, O1 is output, i is the output of the i[th] node in the first layer, x is the input to node i, Ai is a linguistic label from fuzzy set A = (A1, A2, B1, B2,) associated with the node, and {ai, bi, ci} is the premise parameter set used to adjust the shape of the membership function.

B. Layer 2: In this layer the nodes are fixed nodes designated Π, which represent the firing strength of each rule. The output of each node is the fuzzy AND (product or MIN) of all the input signals;

$$O_i^2 = \mu_{Ai}(e)\mu_{Bi}(de), \quad i = 1,2 \qquad (19)$$

C. Layer 3: The output of the layer 3 is the normalized firing strengths. Each node is a fixed rule labelled N. The output of the i[th] node is the ratio of the i[th] rule's firing strength to the sum of all the rules firing strengths:

$$O_i^3 = \overline{w_i} = \frac{w_i}{w_1+w_2} \qquad i = 1,2 \qquad (20)$$

D. Layer 4: The adaptive nodes in the layer4 calculate the rule outputs based upon consequent parameters using the function:

$$O_i^4 = \overline{w_i} f_i = \overline{w_i}(p_i e + p_i de + r_i) \quad i = 1,2 \qquad (21)$$

Where, $\overline{w_i}$ is a normalized firing strength from layer 3, and (pi, qi, ri) is the consequent parameter set of the node.

E. Layer 5: The single node in layer.5 labelled P, calculates the overall ANFIS output from the sum of the node inputs:

$$O_i^5 = \sum_i \overline{w_i} f_i = \frac{\sum_i w_i f_i}{\sum_i w_i} \qquad i = 1,2 \qquad (22)$$

The algorithm of ANFIS MPPT control is shown in Fig 10

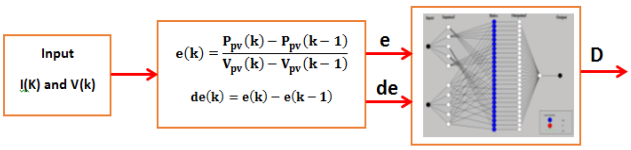

Fig 10. The algorithm of ANFIS MPPT control

7. ANFIS training

Training the ANFIS system with the training data set is shown in the figure1 [20]. The training error is the difference between the training data output value, and the output of the fuzzy inference system corresponding to the same training data input value, (the one associated with that training data output value). The training error records the root mean squared error (RMSE) of the training data set at each epoch.

$$RMSE = \sqrt{\frac{\sum_{k=1}^{n}(y_k - \hat{y}_k)}{n}} \qquad (23)$$

The equivalent neuronal structure proposed in Matlab is shown in Figure 11.

The ANFIS Editor GUI plots the training error versus epochs curve as the system is trained Fig 12 and 13. Testing the trained FIS is shown in Fig 14.The average testing error for the training data set is 0.045474.

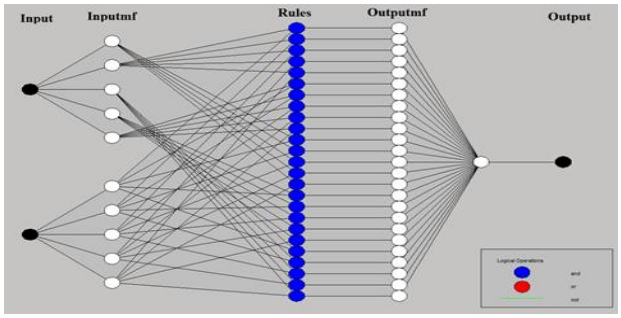

Fig.11 Neuronal Structure of the proposed model in Matlab.

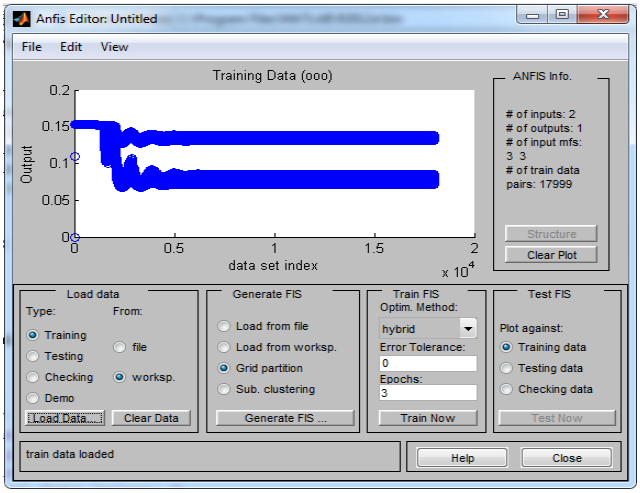

Fig.12 training data (error, changing of error and duty cycler)

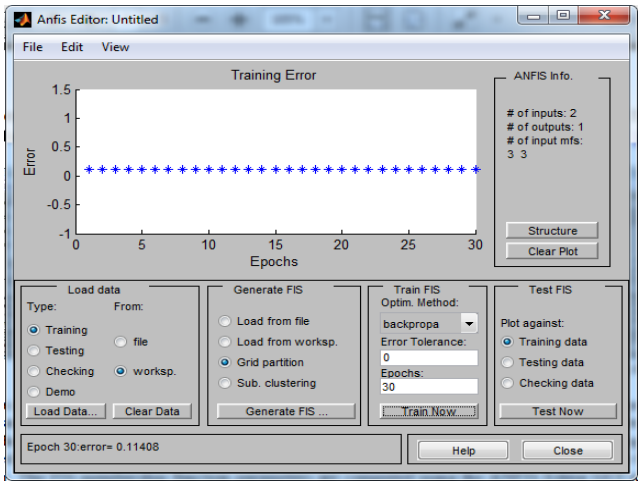

Fig.13 Training error

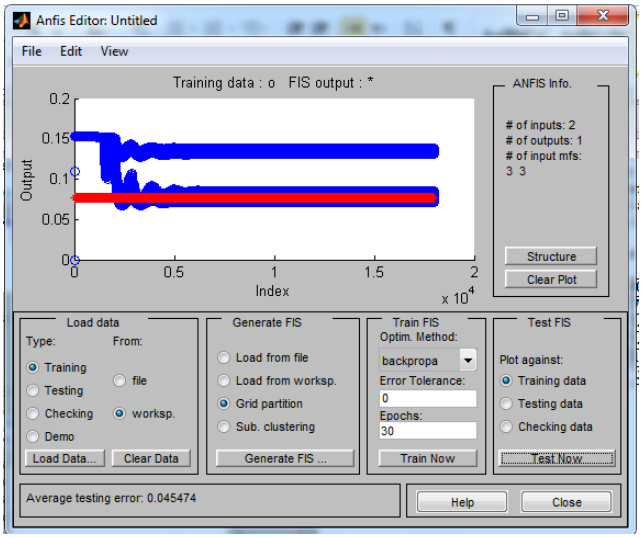

Fig.14 Testing the FIS with Training data set

II. SIMULATION RESULTS AND DISCUSSION

An extensive simulation for both techniques has been done using MATLAB. Some selected results are presented with a comparison between fuzzy and neuro-fuzzy MPPT controllers. The following simulation were presented for different irradiation levels from 200 to 1000 W/m2 at fixed temperature of 25°C as shown in Fig.19-21 and Fig 24-26.

We have chosen a Solarex MSX 60W PV module. It consists of 36 mono-crystalline silicon solar cells connected in series and provides a nominal power 60W. The electrical parameters are given in Table III.

Fig .15 presents I (V) and P (V) Characteristics for PV module (60W) at constant temperature and varying irradiation.
The Fig.16 shows the overall simulation diagram of the proposed system.

Table III *Solarex MSX 60 PV module specifications at 25 ºC*

Typical peak power (P)	**60 W**
Voltage at peak power (VMPP)	**17.1 V**
Current at peak power (IMPP)	**3.5 A**
Short-circuit current (ISC)	**3.8 A**
Open-circuit voltage (Voc)	**21.1 V**
Number of series cells	**36**

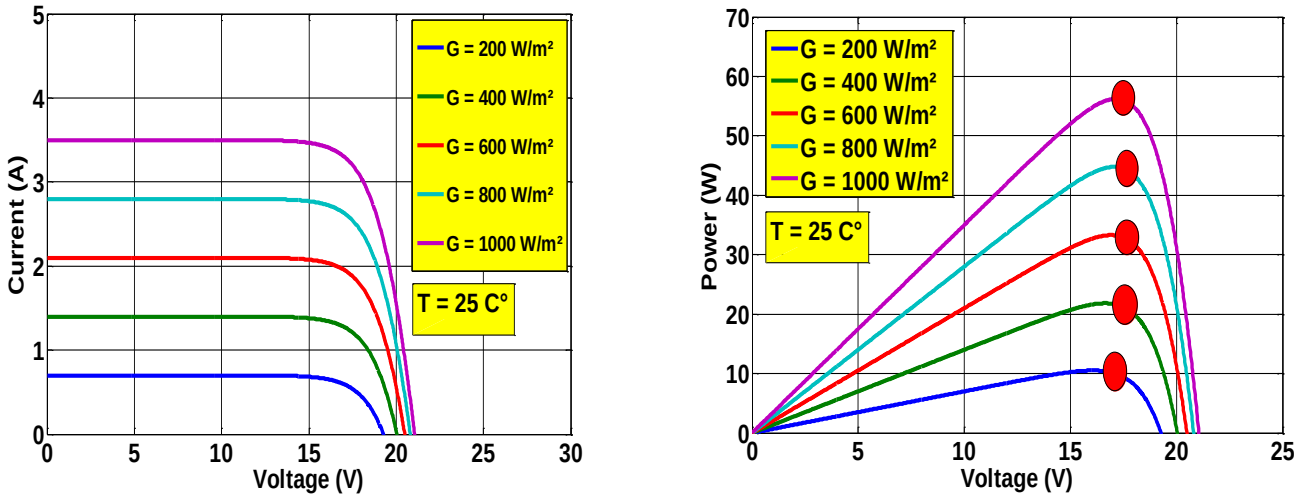

Fig .15. PV Characteristics (60W) at constant temperature and varying irradiation

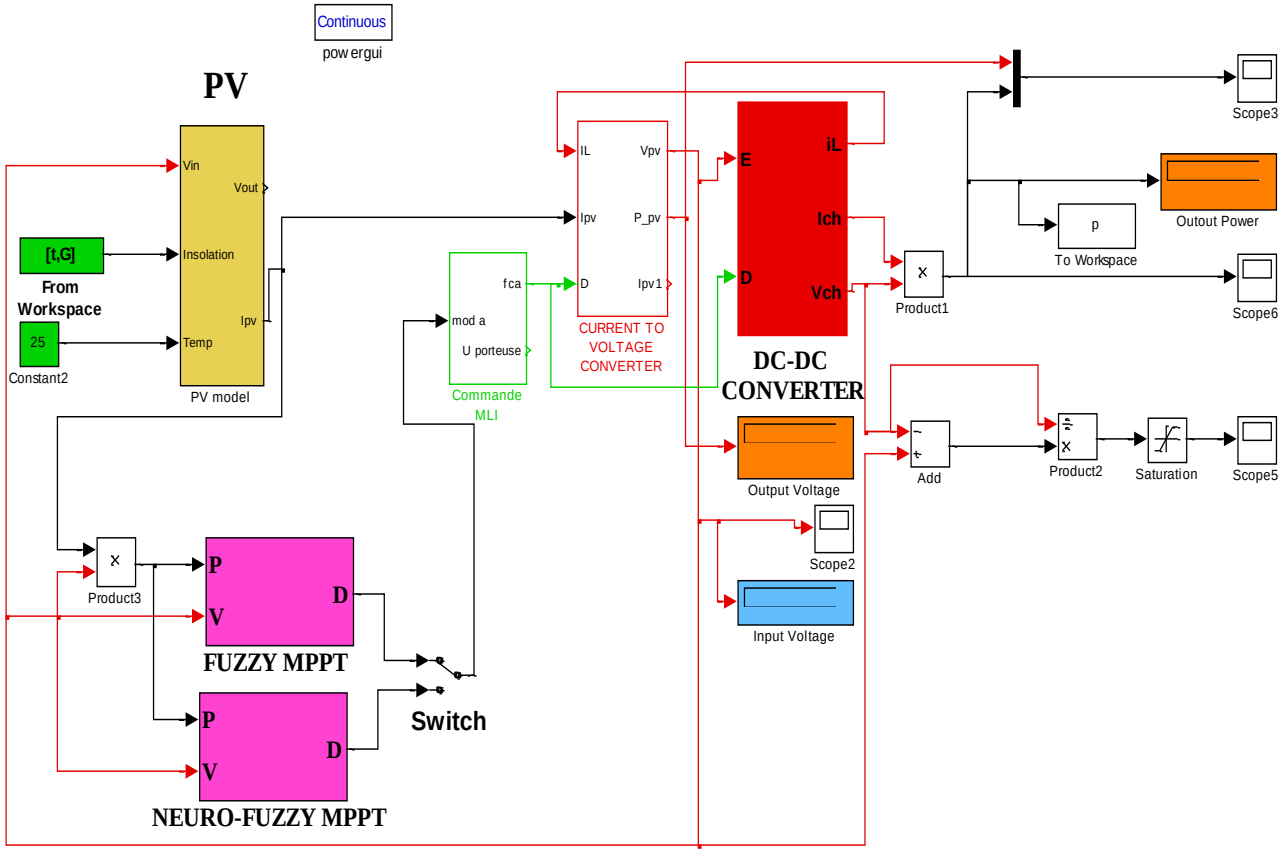

Fig. 16. Block diagram of PV Module with Fuzzy and ANFIS MPPT Controller

A- Fuzzy Logic Control MPPT Strategy

Figure 17 presents the fuzzy Logic MPPT Controller Configuration in matlab/Simulink. Figure 18 shows the evolution of solar irradiance estimated by Liu & Jordan model versus time. We found that the hourly global solar irradiance is more pronounced between 10.00 and 14.00 hours and takes the maximum value at 12.00. A significant deviation in the estimated values has been observed at low sun angle (morning and evening hours), which is of little consequence for solar energy operated systems, because the global radiation during morning and evening hours is very small and constitutes only a small part of the radiation for the day.

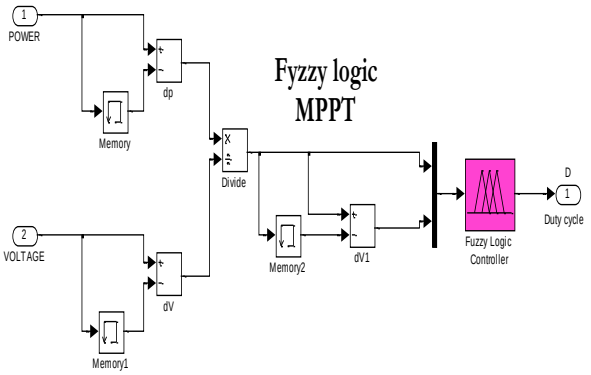

Fig.17 Fuzzy Logic MPPT Controller Configuration in matlab/simulink

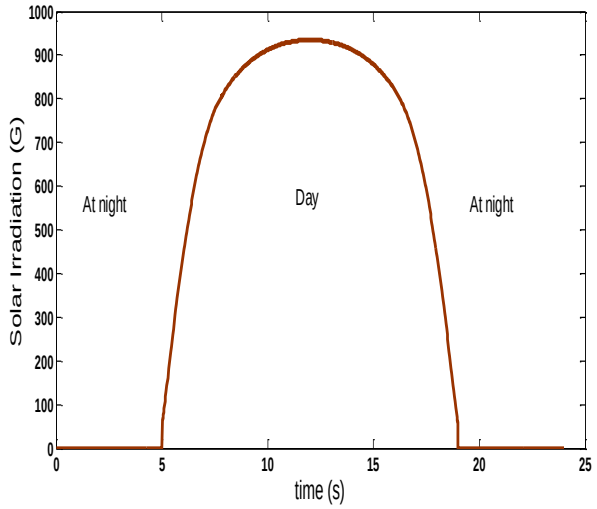

Fig.18. Global irradiation variation profile on inclined plane of Ghardaia site

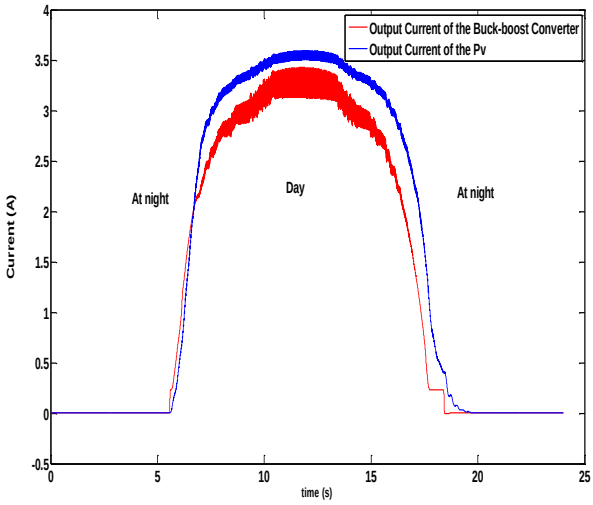

Fig.19 Average hourly current generated by a solar panel and Buck boost converter in a day with Fuzzy MPPT controller

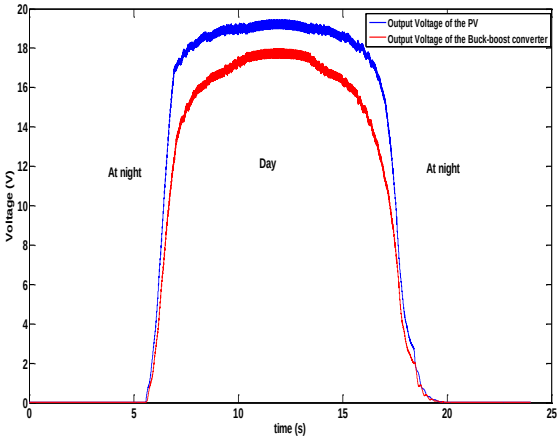

Fig.20. Average hourly voltage generated by a solar panel and Buck boost converter in a day with Fuzzy MPPT controller

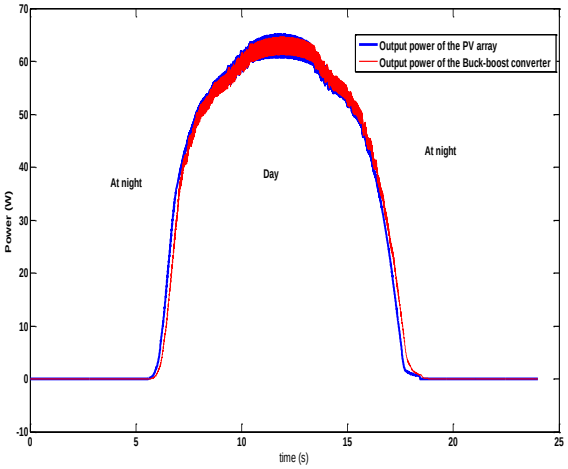

Fig.21. Average hourly power generated by a solar panel and Buck boost converter in a day with Fuzzy MPPT controller

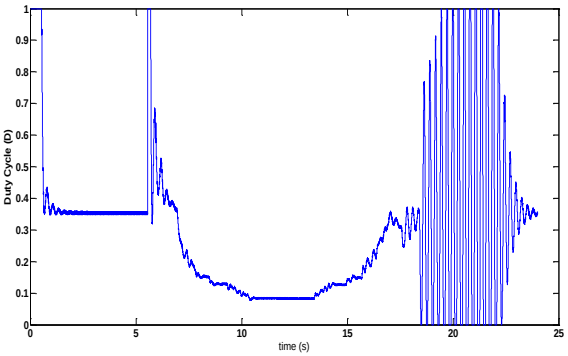

Fig. 22 Duty cycler

From the simulation results, the maximum power point is tracked with excellent simulation results when the radiance fluctuates between t=6h and t=18h for G is between 200W/m^2 and 900W/m^2.

B. ANFIS MPPT controller Strategy

The ANFIS structure information is given in Table IV. Figure 23 shows the evolution of solar irradiance estimated by Liu & Jordan model versus time. We found that the hourly global solar irradiance is more pronounced between 10.00 and 14.00 hours and takes the maximum value at 12.00. A significant deviation in the estimated values has been observed at low sun angle (morning and evening hours), which is of little consequence for solar energy operated systems, because the global radiation during morning and evening hours is very small and constitutes only a small part of the radiation for the day.

Table IV *the ANFIS structure information*

Number of nodes	**35**
Number of linear parameters	**27**
Number of nonlinear parameters	**18**
Total number of parameters	**45**
Number of training data pairs	**17999**
Number of checking data pairs	**0**
Number of fuzzy rules	**9**

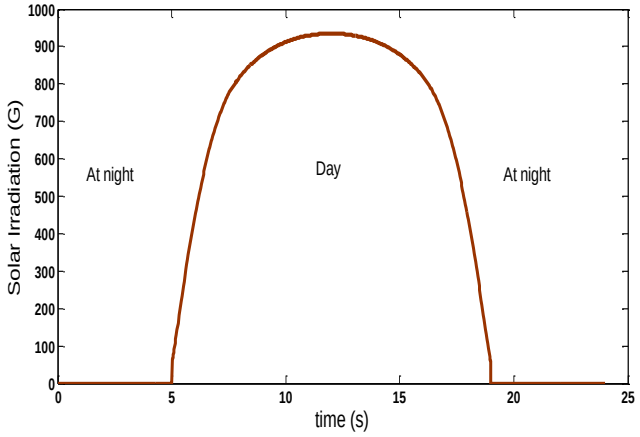

Fig.23. Global irradiation variation profile on inclined plane of Ghardaia site

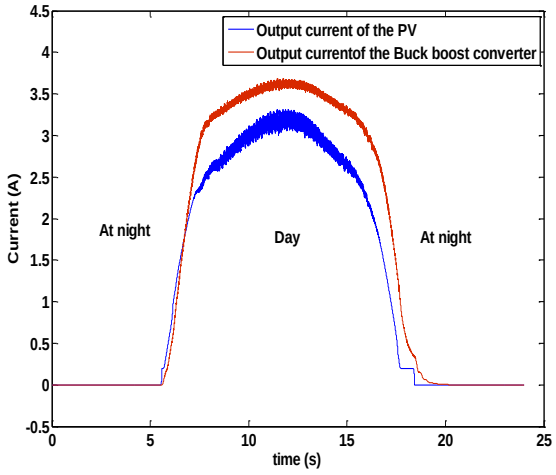

Fig.24. Average hourly current generated by a solar panel and Buck boost converter in a day with Neuro-fuzzy MPPT controller

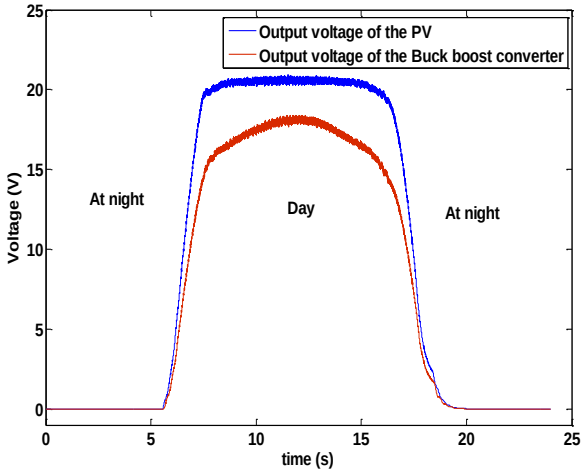

Fig.25. Average hourly voltage generated by a solar panel and Buck boost converter in a day with Neuro-fuzzy MPPT controller

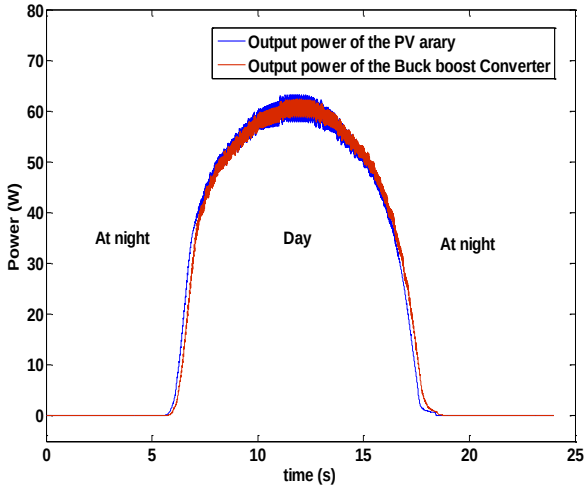

Fig.26. Average hourly power generated by a solar panel and Buck boost converter in a day with Neuro-fuzzy MPPT controller

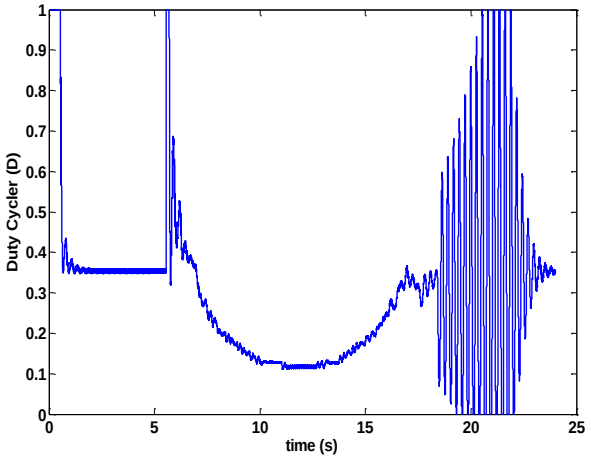

Fig. 27 Duty cycler

From the simulation results, the maximum power point is tracked with excellent simulation results when the radiance

fluctuates between t=6h and t=18h for G is between 200W/m^2 and 900W/m^2.

As shown Neuro-fuzzy controller shows smother power signal line, less oscillating and better stable operating point than fuzzy controller .From the simulation results, it can be deduced that the Neuro-fuzzy controller has better performance than fuzzy controller, and it has more accuracy for operating at MPP.

III.CONCLUSION

This paper has presented a mathematical model to estimate the various components of solar radiation received in the site of Ghardaia on inclined plane using the model of Liu & Jordan, developed in Matlab/Simulink environment. The variation of incidence solar radiation and temperature were found to be the main cause of modification in the amount of PV generator power output.

In the present work, we studied two techniques ,fuzzy and neuro-fuzzy strategy of maximum power tracking in order to compare them and to control the voltage of the solar panel in order to obtain the maximum power possible from a PV generator, whatever the solar irradiation and temperature conditions. We have shown through the simulation of the photovoltaic system in Simulink, the neuro- fuzzy controller technique under variable irradiation conditions is much more reliable and robust and has satisfactory results and present no oscillations in permanent state.

REFERENCES

[1] Ali Khodja M. «*Sauvegarde des tissus anciens à travers la réhabilitation des maisons traditionnelles cas de la vallée du M'Zab*», International Conference on Medina, Tlemcen, Algeria, 13-14 May; 2008.

[2] I. Hadj Mahammed, A. Hadj Arab, F. Youcef Ettoumi, S. Berrah, A. Boutelhig and Y. Bakelli , «*A Comparative Study to Select a Mathematical Model for IV Characteristics Accuracy under Outdoor Conditions*», sienr 2010 ghardaia.

[3] S. Semaoui a, A. Hadj Arab, S. Bacha , B. Azoui , «*The new strategy of energy management for a photovoltaic system without extra intended for remote-housing*», Solar Energy 94 (2013) 71–85.

[4] Smail Semaoui, A. Hadj Arab ,Seddik Bacha, Boubakeur Azoui, «*Optimal Sizing of a Stand-alone Photovoltaic System with Energy Management in Isolated Areas*» ,Energy Procedia 36 (2013), 358-368.

[5] M. El-yadri, R. Saadani, Li. Zorkani and M.Rahmoune, «Propre.Ma" project: Modeling and simulation of Grid connected photovoltaic system for Meknes Climate»,2nd International Renewable and Sustainable Energy Conference IRSEC14, Ouarzazate, Morocco – October 17-19, 2014

[6] M. Merad Mersi, A. Cheknane et M. Rougab Ilyse, «*Introduction au gisement solaire algérien théorie et application*», université Amar Telidji- Laghouat.

[7] A. Mellit et S. A. Kalogirou, « *ANFIS-based modelling for photovoltaic power supply system: A case study* », Renewable Energy, vol. 36, no. 1, p. 250–258, janv. 2011.

[8] F.Belhachat, C. Larbes, L. Barazane, S. Kharzi, « *Commande neuro-floue d'un hacheur MPPT* », 4th international conference on computer integrated manufacturing, CIP'2007.

[9] L.K. Lettinga, J.L. Mundaa, Y. Hamama, «Optimization of a fuzzy logic controller for PV grid invertercontrol using S-function based PSO», Solar Energy Volume 86, Issue 6, June 2012, Pages 1689–1700.

[10] Adel Mellit, Soteris A. Kalogirou «MPPT-based artificial intelligence techniques for photovoltaic systems and its implementation into field programmable gate array chips: Review of current status and future perspectives», Energy Volume 70, 1 June 2014, Pages 1–21.

[11] Mhamed Rebhi , Ali Benatillah , Mabrouk Sellam , Boufeldja Kadri, «*Comparative Study of MPPT Controllers for PV System Implemented in the South-west of Algeria*», Energy Procedia 36 (2013) 142 – 153

[12] S .Lalouni, D. Rekioua, « *Optimal Control of a Grid Connected Photovoltaic System with Constant Switching Frequency* », Energy Procedia 36 (2013) 189 199.

[13] H.E.A. Ibrahim, Mahmoud Ibrahim, «*Comparison Between Fuzzy and P&O Control for MPPT for Photovoltaic System Using Boost Converter*», Journal of Energy Technologies and Policy, Vol.2, No.6, 2012.

[14] N. Drir 1 , L. Barazane 1 and M. Loudini, «*Fuzzy logic for tracking maximum power point of photovoltaic generator*», Revue des Energies Renouvelables Vol. 16 N°1 (2013) 1 – 9.

[15] Swati Singh1, Lini Mathew2, Shimi S.L.3, «*Design and Simulation of Intelligent Control MPPT Technique for PV Module Using MATLAB/ SIMSCAPE*», International Journal of Advanced Research in Electrical,Electronics and Instrumentation Engineering, Vol. 2, Issue 9, September 2013.

[16] Ridha Benadli, Anis Sellami,«*Sliding Mode Control of a Photovoltaic-Wind Hybrid System*», internationale conference on electrical sciences and technologie in Maghreb,CISTEM 2014.

[17] Petr Hušek , Otto Cerman, « *Fuzzy model reference control with adaptation of input fuzzy sets* », Knowledge-Based Systems 49 (2013) 116‑122.

[18] Amitava Chatterjee, Ranajit Chatterjee, Fumitoshi Matsuno, Takahiro Endo, « *Augmented Stable Fuzzy Control for Flexible Robotic Arm Using LMI Approach and Neuro-Fuzzy State Space Modeling*», IEEE Transactions on Industrial Electronics, vol. 55, no. 3, pp. 1256-1270, 2008.

[19] Radu-Emil Precup, Stefan Preitl, Mircea-Bogdan R˘adac, Emil M. Petriu, *Fellow, Claudia-Adina Dragos, József K. Tar*« *Experiment-based teaching in advanced control engineering*», IEEE Transactions on Education, vol. 54, no. 3, pp. 345-355, 2011.

[20] Zhifei Chen, Sara Aghakhani, James Man, and Scott Dick, «ANCFIS: A neuro-fuzzy architecture employing complex fuzzy sets», IEEE Transactions on Fuzzy Systems, vol. 19, no. 2, pp. 305-322, 2011.